IRIS AperTO

UNIVERSITÀ DEGLI STUDI DI TORINO

AperTO - Archivio Istituzionale Open Access dell'Università di Torino

Human aromatase: perspectives in biochemistry and biotechnology

This is the author's manuscript

Original Citation:

Availability:

This version is available http://hdl.handle.net/2318/127987 since 2016-05-25T14:59:37Z

Published version:

DOI:10.1002/bab.1088

Terms of use:

Open Access

Anyone can freely access the full text of works made available as "Open Access". Works made available under a Creative Commons license can be used according to the terms and conditions of said license. Use of all other works requires consent of the right holder (author or publisher) if not exempted from copyright protection by the applicable law.

(Article begins on next page)

19 April 2024

UNIVERSITÀ DEGLI STUDI DI TORINO

This is the accepted version of the following article:

[Di Nardo, G. and Gilardi, G. “Human aromatase: perspectives in biochemistry and biotechnology”, Biotechnology and Applied Biochemistry (2013), 60(1), 92-101.],

which has been published in final form at [http://onlinelibrary.wiley.com/doi/10.1002/bab.1088/abstract]

Human aromatase: perspectives in biochemistry and biotechnology

Giovanna Di Nardo and Gianfranco Gilardi*

Department of Life Sciences and Systems Biology, University of Torino, via Accademia Albertina 13, 10123 Torino, Italy

* Author to whom correspondence should be addressed;
E-Mail: gianfranco.gilardi@unito.it;
Tel.: +39-011-670-4593; Fax: +39-011-670-4643.

Abstract

Aromatase (CYP19) is involved in steroidogenesis catalysing the conversion of androgens into estrogens through a unique reaction that causes the aromatization of the A-ring of the steroid. The enzyme is widely distributed and well conserved among species as it plays a crucial role in physiological processes such as control of reproduction and neuroprotection.

It has also been subject of intense research both at the biotechnological level in drug development due to its involvement in estrogen-dependent tumors and at a fundamental biochemical level as there are numerous questions regarding its reaction mechanism. This review will report on the great progress made in this area.

1. Introduction

Aromatase (CYP19) is involved in the conversion of androgens into estrogens in the last step of steroidogeneis [1-3]. The conversion of androgens into estrogens by mammalian tissues was first observed in the 1950s [4-6], coinciding with the discovery by K. Ryan that this process in microsomes of human placenta is associated with a requirment for NADPH and oxygen [7]. The role of aromatase in producing higher levels of estrogens in breast cancer cells compared to non-cancerous cells [8] has led to numerous studies towards the development of inhibitors for theurapeutic purposes. The historical background and the main discoveries in the field of sexual steroids, aromatase and aromatase inhibitors (AIs) have been extensively reviewed by Santen and co-workers [9].

In the meanwhile, different groups have tried to develop a recombinant system for the biochemical characterization of the enzyme; this review reports on the progress made over the last few years in the elucidation of the structure-function relationship in this unique cytochrome P450.

2. Evolutionary considerations

Aromatase appears in an early divergent chordata, the cephalochordate amphioxus (the Florida lancelet, *Branchiostoma floridae*) [10] where as in most living organisms, it is found as a single isoform. However, there are two exceptions, represented by Teleosts, where 2 isoforms have been described [11] and pigs, where 3 isoforms have been observed [12].

Sequence alignment between 169 non-redundant members of the aromatase family [13] and phylogenetic analysis [14] shows that the protein sequence is well conserved among species. Although the N-terminal transmembrane domain and the C-terminus show some divergences, most of the internal sequences are well conserved. Furthermore, some important regions for substrate accommodation (F-G loop) and residues forming the active site are highly conserved [15].

A DIVERGE analysis has also shown that there is little functional divergence in the CYP19 family [14], in contrast to what has been reported for other P450 families, such as CYP3 [16].

This observation leads to the question: why has aromatase evolution not diverged, producing different isoforms in most organisms?

The presence of a single isoform of aromatase in humans is not advantageous from a theurapeutic point of view: as its distribution is quite broad, the use of aromatase inhibitors as anti-cancer drugs is limited by the fact that all the protein present in different tissues of the body will be affected by these molecules. This leads to serious side effects: for example, collateral inhibition of brain aromatase with consequent reduction of cognitive functions has been reported in post-menopausal women treated for breast cancer [17].

3. Distribution

Aromatase is expressed by gonadal tissue and brain in vertebrates and it is essential for reproduction and fertility [3,18,19]. In primates and artiodactyls it is also highly expressed in placenta. In humans, aromatase can be found in many tissues including gonads, brain, adipose tissue, placenta, blood vessels, skin, bone and endometrium [20].

There has been large interest in studying aromatase in mammalian brain since this enzyme has been found in many regions of this organ. In the early 1970s, it was demonstrated that the brain neuroendocrine tissues were able to convert androgens to estrogens, suggesting the possibility that many effects of gonadal androgens on neural cell function could be mediated by local conversion to estrogens by the activity of aromatase [21]. More recently, high levels of expression have been detected within the bed nucleus of the stria terminalis, the hippocampus, the amygdala, several hypothalamic nuclei, the medial preoptic area, the nucleus accumbens and in several regions of the cortex [22]. It is also very interesting that aromatase has been demonstrated to play a crucial role not only in the regulation of sexual differentiation and of reproduction during adult life [23,24], but also in other physiological and behavioural processes, including neuroplasticity, cell growth, migration and neuroprotection against degeneration and brain injury

[25]. Furthermore, the central role of aromatase in neuroprotection has been demonstrated in the cases of stroke [26], Alzheimer's and Parkinson's diseases and epilepsy [27-29].

These findings point out how important the presence of more than one member in the aromatase family would have been for therapeutic purposes i.e. targeted inhibition for controling estrogen biosynthesis in specific tissues.

4. Catalytic mechanism of aromatase reaction

The physiological substrates of aromatase are androstenedione, testosterone and 16alpha-hydroxytestosterone that are converted into estrone, 17beta-estradiol and 17beta, 16alpha-estriol, respectively (Figure 1). Very recently, it has been reported that the enzyme is able to convert dihydrotestosterone, a more potent androgen than testosterone, into a series of products including 19-hydroxy- and 19-oxo derivatives and the resulting norsteroid products deriving from the loss of 19-methyl group [30]. Furthermore, aromatase possess estrogen 2-hydroxylase activity [31].

The conversion of androgens into estrogens is a three-step reaction, each requiring one mol of oxygen and one mol of NADPH. The electrons are shuttled from NADPH to heme through the redox partner, cytochrome P450-reductase (CPR).

The first two steps of the reaction are hydroxylations of C19, that produce 9-hydroxy and 19-oxo as stable intermediates. The third step consists in the removal of C19 as formic acid and the aromatization of the steroid A-ring, unique to aromatase [1,3].

The biochemistry of the last step is still unclear and many studies have been carried out in order to elucidate it.

The removal of the 1*β* and 2*β* hydrogens from 19-oxoandrostenedione and their incorporation into water during the third step of catalysis was established by using isotopically labeled substrates [32-34]. It was also proven that one oxygen atom is incorported into formate [35].

A key question is which of the intermediates of the classic P450 catalytic cycle is responsible for the aromatization step. One proposal (Figure 2A) is that the ferric peroxide species of the P450 ($FeOO^{-}$) gives a nucleophilic attack to the

carbonyl group of the aldehyde [35]. The peroxide fragmentation and the abstraction of the 1*β* proton from the steroid result in the aromatization of the A-ring of the steroid molecule with the release of formic acid. In such a mechanism, one oxygen atom is therefore incorporated into the formic acid.

A second mechanism (Figure 2B) proposed for the final step of aromatization suggests that the reactive P450 species is the "Compound I", responsible for 1*β*-hydrogen subtraction from a *gem*-diol intermediate. One electron is then transferred from the A-ring to the iron ($Fe^{3+}OH$) and a second hydrogen is subtracted from the *gem*-diol causing the release of the C19 as formic acid [36]. This mechanism is not supported by the experimental data showing that one oxygen atom is incorporated into the formate. However, the authors argue that 19-hydroxy- and 19-oxoandrostenedione metabolites can have been produced by cytochromes P450 different from aromatase when microsomal preparations were used for the $^{18}O_2$ incorporation studies [35].

New insights on the catalytic mechanism came from the crystal structure of aromatase in complex with the substrate androstenedione [37]. A key catalytic role was assigned to Thr310-Ala306 pair that performs a nucleophilic attack on C2-*β*, followed by an electrophilic attack on the C3 keto oxygen by a protonated Asp309 to promote C2-*β* abstraction and 2,3-enolization.

Very recently, molecular dynamics and hybrid quantum mechanics/molecular dynamics (QM/MM) simulations were used to explore possible pathways for the ferric peroxo intermediate ($Fe^{3+}O_2^{2-}$) to act on 19-oxoandrostenedione and initiate aromatization [38]. In the most kinetically advantageous mechanism (Figure 2C), the peroxo-species attacks the aldehyde causing the cleavage of the C10-C19 bond through the formation of a transient peroxohemiacetal intermediate. Then, a peroxoformate intermediate is formed and the heterolytic cleavage of the O-O bond releases formate and generates the ferryl ($\bullet Fe^{4+}=O$) Compound I species in an analogous manner to Compound I formation driven by peracids. The latter yields Fe^{3+}–OH by overall *1β*-hydride abstraction which may occur via the series of 2- electron movements shown in Fig. 2C. Alternatively, initial hydrogen atom abstraction can be followed by electron transfer oxidation of the C1-based radical by the Compound II (Fe^{4+}–OH) species to give the C1-carbocation that undergoes proton abstraction by the Asp309 carboxylate at C3 to form the ketone, with concomitant shifts of

the double bonds. In the last step, abstraction of the *2β*-proton leads to stereoselective enolization and formation of the aromatic system [38].

Ghosh and colleagues [37] propose that Asp309 forms a hydrogen bond with the 3-keto moiety of the substrate and this residue is predicted to have a pK_a of 7.7 [38], which is mainly protonated at physiological pH. This residue is suggested to be involved not only in the proton relay network but also in the gating of the proton for substrate aromatization. This proton gating mechanism is proposed to be a control mechanism allowing the stabilization of the different reaction intermediates responsible for the three step of catalysis [38].

A key question about the reaction of aromatase is the processive *versus* the distributive mechanism. In 2010, pulse-chase experiments with radiolabeled androstenedione and the products of the first two steps of reaction, 19-hydroxy and 19-oxo-androstenedione, showed a decrease in radiolabeled estrone when the two intermediates were introduced in the reaction mixture [39,40]. These data suggest the lack of processivity and therefore a distributive kinetic model was built based on the rate constants of the three steps of aromatase reaction, the dissociation constant for the substrate androstenedione and the 19-hydroxy and 19-oxo, pre-steady-state ligand binding experiments and iron reduction rates [39,40].

5. Expression in recombinant systems, purification and spectroscopic characterization

Several groups have tried to develop a recombinant system for high level expression of human aromatase in bacteria [41-46] or insect cells [47-49] followed by a purification protocol resulting in a stable and active form of the enzyme. Many problems have been encountered mainly due to the presence of the protein in inclusion bodies and the necessity of a ligand addition (substrate or inhibitor) to stabilize the protein and prevent heme loss during the purification. Once purified, the tight binding of the ligand used during purification causes further difficulty in fully removing it and therefore obtaining a single spectroscopic species. Our group has developed a robust recombinant bacterial system resulting in large quantities of pure protein

which had led to the first crystal structure of a recombinant form of human aromatase (in collaboration with Prof. Debashish Ghosh, data not yet published).

5.1 UV-vis spectroscopy

The spectral properties of aromatase have been reported by different groups. In the oxidized state, the Soret maximum of the purified protein in the absence of ligand is detected at 417 nm [50-51] whereas in the androstenedione complex the signal shifts to 394 nm indicating a typical Type I spectrum. A typical Type II binding spectrum with the main Soret peak detected at 422 nm was observed in the recombinant protein in complex with letrozole [45] and anastrozole [52].

The substrate induced spectral transition (shift from 417 to 394 nm) was also detected in the recombinant form of aromatase incorporated in nanometer scale phospholipids bilayers (Nanodiscs) [51]. In the latter work, the oxy-ferrous complex was obtained by mixing an anaerobic sample of the ferrous enzyme with oxygen-saturated buffer in a stopped- flow system. This intermediate is more stable than the one observed for P450 3A4 [53] and showed a Soret peak at 418 nm, with the characteristic split hyperporphyrin Soret and Q-band at 555 nm [54] as already oberved for the oxy-ferrous intermediates of other P450s [55]. The auto-oxidation decay that produces the ferric resting state with the release of a superoxide anion [56] was also observed and rate constants of 0.21 s^{-1} at 25 °C and 0.7 s^{-1} at 37 °C were measured from the spectral decay [51].

Temperature derivative spectroscopy has also been used to determine the energy of activation for the conversion of oxy-ferrous CYP19A1, saturated with androstenedione, to ferric CYP19A1 (17.5 kcal/mol) with a rate constant of 0.02 s^{-1} at 298 K [57]. High activation energy barriers for autoxidation are typical of cytochromes P450 and are in line with the idea that these enzymes do not have a well-defined channel for molecular oxygen entry in the active site [57].

5.2 EPR spectroscopy

EPR spectroscopy has been applied to characterize the iron spin state when aromatase is ligand-free, in complex with the substrate or in complex with the inhibitor anastrozole [52,54].

It has been noticed that, in the substrate free form, there are two distinct low spin species whereas single high spin and low spin species are detected in the presence of the substrate androstenedione and the inhibitor anastrozole, respectively [52,54].

Experimental insights in the reaction mechanism of aromatase came from the cryoreduction of the oxy-ferrous complex at 77 K and the consequent generation and characterization of the peroxo-ferric species. This intermediate can be distinguished by EPR from the hydroperoxo-ferric one, usually obtained after cryoreduction of cytochromes P450 at 77 K [58,59]. It was found that, in human aromatase, in contrast with other P450s, the peroxo-ferric species is the primary CYP19 intermediate observed at 77 K after cryoreduction [54]. The protonation of the peroxo-ferric intermediate is somehow hindered, stabilizing this species that can therefore perform the nucleophilic attack on the aldehyde group present on the 19-oxoandrostenedione in the last step of the reaction. These EPR spectroscopic findings support the recent mechanism proposed by Akthar and co-workers [35] and Sen and Hackett [38] for the third step of the aromatization reaction, as discussed in Section 4.

We recently characterized the complex aromatase-anastrozole by means of ^{14}N HYSCORE spectroscopy. We demonstrate that the binding of the inhibitor is occurring *via* N4 of the triazole ring that directly coordinates the iron atom [52].

5.3 Resonance Raman spectroscopy

The heme active site of human aromatase with and without substrate was characterized by RR spectroscopy using the Fe-CO ($\nu_{Fe\text{-}CO}$) and the Fe-S ($\nu_{Fe\text{-}S}$) associated vibrations as structural markers [50]. Also in this case, the experimental evidence supports the mechanisms in which the peroxo-

intermediate is the one involved in the third step of aromatization (Figure 2A and 2C). In fact, according to the experimental data, heme distal site is very flexible and the presence of the substrate perturbs the heme environment when bound to aromatase. From the CO-associated vibrations, it turned out that the binding of 19-oxo-androstenedione, the product of the second step of reaction, might perturb the proton shuttle machinery responsible for compound I formation, and stabilizes the ferric-peroxo species in the third oxidative step. Since the first two hydroxylation steps are believed to proceed through the "classical" P450 catalytic cycle, the authors hypothesized that the different substrates/intermediates can modulate the structure of both distal and proximal sites in a different way therefore stabilising different intermediates [50].

6. Crystal structures of human aromatase

The first crystal structure of human aromatase was published in 2009 and was obtained from the enzyme directly extracted and purified from placenta [37]. The structure was solved in complex with the substrate androstenedione at a resolution of 2.9 Å and recently refined to 2.75 Å [60]. Human aromatase shares the typical fold of cytochromes P450, consisting of 12 alpha helices (A-L) and 10 beta strands (1-10). Interestingly, an additional β strand-like element is present at the N-terminal.

The substrate binding pocket of aromatase is considerably smaller (400 $Å^3$) when compared to other P450s such as 3A4 and 2D6 (both 530 $Å^3$). This is responsible for the strict substrate specificity. A distortion of helix I caused by Pro308, a residue unique to aromatase among all the other P450s, creates the space for substrate accommodation (Figure 3). A number of residues such as Arg115, Ile133, Phe134, Phe221, Trp224, Ala 306, Thr310, Val370, Val373, Met374, Leu477 form van der Waals contacts with androstenedione, which tightly fits in the catalytic pocket. The distortion of helix I places the 3-keto group of androstenedione close by 2.6 Å from the carboxylate $O_{\delta 2}$ of the Asp309 side chain so that it can form a H-bond. Furthermore, the H2*β*

hydrogen of the A-ring of bound androstenedione is very close to the Ala306-Thr310 pair that is implicated in all three hydroxylation steps.

Very recently, Ghosh and co-workers solved the structure of the enzyme in complex with the steroidal inhibitor exemestane and two new inhibitors with a stronger anti-proliferative effect in MCF-7 breast cancer cell line [60]. These structures are very similar to the one in complex with the substrate androstenedione, with a root mean square deviation (RMSD) of 0.3 Å for the backbone atoms. Some conformational changes are only present at the entrance of the substrate access channel in relation to the accommodation of the different ligands [60]. The structural basis for the potent inhibitory effect given by two new compounds are provided by the fact that although the steroid scaffold binds similarly to the substrate androstenedione, the newly introduced side groups occupy the access channel stabilising the bound form of the enzyme [60].

7. Active site residues important for catalysis: site-directed mutagenesis studies

The catalytic cleft of aromatase seems to be optimized for a very tight substrate binding, with measured K_M values in the nM range. Site directed mutagenesis has been used to study the importance of specific amino acids for substrate or inhibitor binding and catalysis [41,45,61-65]. Table 1 summarizes the residues that have been targeted for mutagenesis studies, their role according to the crystal structure, the mutants generated and the corresponding variations in the catalytic parameters toward androstenedione compared with the wild-type protein. The location of some critical residues for catalysis is shown in Figure 3. For example, the crucial role of Asp309, suggested to be involved in the proton relay network for substrate aromatization, is well known since the mutants D309N and D309A created in a Chinese hamster ovary (CHO) cell line displayed a significant reduced activity respect to the wild-type [64].

The importance of some residues forming van der Waals contact with the substrate androstenedione, such as I133, F221, W224, and M374 was also investigated by site directed mutagenesis. Although some contrasting data

were reported depending on the experimental system used (in cell or microsomal assay), significant changes in K_M and/or k_{cat} values were measured when these residues were mutated (Table 1 and Figure 3). The data give further evidence to the idea that aromatase catalytic cleft is higly optimized for androgen binding, accommodation and catalysis.

8. Aromatase-CPR interaction

The interaction of aromatse with its electron-donating partner cytochrome P450 reductase (CPR) has been studied by kinetics experiments and docking methods.

As soon as the first crystal structure of aromatase was published [37], computational methods were used to calculate the surface electrostatic potential of the protein since it is known that the FMN-binding domain of CPR contains carboxylate groups, confering a negatively charged surface that forms ion pairs with basic residues on a positively charged face of P450s [66-68]. In a first docking model based on the crystal structures of aromatase (PDB ID: 3EQM) and CPR (PDB ID: 1AMO) this typical charge interaction was confirmed since the proximal surface of aromatase is positively charged [15].

In a step-wise and flexible docking approach, aromatase was docked to the FMN binding domain of CPR and its FAD and NADPH binding domains were added afterwards [69]. The model of aromatase-CPR complex shows that the distance between the FMN and the heme is 18.8 Å, consistent with data available for P450 BM3 [70]. Furthermore, based on sequence alignment, the authors identified five positively charged amino acids on the aromatase sequence (K99, K108, K389/K390, K420 and R425) aligning with residues of different cytochromes P450 already known to interact with negatively charged residues present on the CPR surface [67,71,72]. The model of aromatase-CPR complex shows that residue K108, part of the helix B' of aromatase, intrudes into a cleft between the FMN and FAD-binding domains, interacting with residues N175/T177 of CPR. This result was validated by experimental data showing that the mutant K108Q, generated in a recombinant system

shows a 20-fold increase in the K_M value for CPR with respect to WT. Both WT and the mutant K108Q were expressed in CHO cells, and a lower aromatase activity was detected in the case of the mutant, suggesting a key role for K108 in promoting electron transfer from CPR to aromatase [73].

Aromatase-CPR interaction might be influenced by possible post-translational modifications on the proximal site of the cytochrome P450. It has been demonstrated that the residue Tyr361 can be phosphorylated in breast cancer cell lines [74], leading to an increase of aromatase activity. This result is unexpected since a phosphorylation introduces negative charges on the aromatase proximal site, resulting in a decrease in CPR affinity. It has also been proposed that a self-association of aromatase monomers involving the proximal site of the enzyme [75] and leading to an oligomeric assembly would prevent the binding of kinases and the phosphorylation of Tyr361. This hypothesis is very interesting and needs further investigation together with a deeper study on the effect of Tyr phosphrylation on the coupling with CPR.

9. Membrane integration and substrate access channel

The crystal structure of human aromatase and the sequence alignment with other mammalian P450s suggest that the enzyme has a N-terminal membrane-integrating sequence longer than that present in other mammalian cytochromes P450 [15,37].

Based on a hydrophobicity plot, Gosh and co-workers [37] predicted that the membrane integration involves residues 21–42 and 49–71 and that the N-terminus, carrying the glycosylation site Asn12, is protruding in the lumen [76]. The model suggests that helix A' (residues 57–68) and part of helix A (residues 69–80) are embedded in the membrane placing the entry of the substrate access channel at the protein/lipid interface [37]. This is consistent with the lipophilic nature of the substrates that aromatase can accommodate through a tunnel partially formed by F-G and β8-β9 loops. Molecular dynamics simulations also suggested that the F-G loop is a flexible region of the protein [77]. In this work, a model based on weak experimental electron density map was built showing the N-terminal transmembrane helix projecting out from the protein into the lipids. The transmembrane segment was

suggested to interact with the corresponding transmembrane segment of CPR and the active site access is at the protein/lipid interface [77].

In another computational study, a model was proposed where A, A′, G′, and K′ helices and the sheets 1, 2, 8, and 9 are in contact with the membrane. This study showed that a clear preferential pathway for androstenedione binding and release is present only in the MD simulations performed with the protein embedded in the membrane [78]. The latter would stabilize the pathway corresponding to the "Solvent channel" previously detected in other P450s [79].

10. Dynamics and flexibility

Molecular dynamics simulations were recently applied to study the flexibility of aromatase using normal mode analysis (NMA) in combination with elastic network (EN). The data show that the enzyme has a rigid core with a compact active site even when bound to the membrane, with a certain degree of flexibility limited to the ligand access channel [77]. However, the available crystal structures are of the enzyme in complex with steroidal molecules. Further structural studies on the substrate-free form of the enzyme are required to confirm the degree of rigidity of aromatase.

The analysis of the dynamics of the protein shows that the enzyme possesses a rigid core both in the presence and the absence of the substrate. The most flexible regions are H-I, D-E, G-H′ and F-G loops. The average root mean square fluctuation (RMSF) values for different regions of the protein were calculated both in the absence and presence of the substrate. The heme cofactor, the catalytic site and the inner core of the protein show RMSF below the average fluctuation of the molecule. The putative access channel and the proximal cavity have higher RMSF values than heme, the catalytic cleft and the inner core. After substrate removal, the rigidity of the catalytic cleft does not seem to be affected whereas the access channel and the inner core of the protein show an increase in RMSF [77].

These computational simulations are supported by Raman spectroscopy that could detect specific substrate-induced structural changes in the heme pocket [50].

Our group used ATR-FTIR spectroscopy to follow the dynamics and flexibility of human aromatase and a significant decrease in the flexibility of α-helices was measured in the presence of the substrate androstenedione and the inhibitor anastrozole. Furthermore, time resolved fluorescence experiments allowed to measure Trp fluorescence lifetimes and to identify a change in the dynamics of the helix F upon ligand binding (manuscript submitted). Helix F is part of the substrate access channel, where a "breathing" movement has been suggested to take place to allow ligands to enter the catalytic pocket [77].

The question of how the enzyme conformation changes when a substrate or inhibitor binds remains unsolved and would be crucial for the design of new inhibitors.

11. Conclusions

Aromatase has been the subject of intense studies since it was discovered in the 1950s, however its biochemistry requires further studies. Important aspects mainly regarding the third step of its catalytic reaction and the flexibility of this important enzyme still need further investigation in order to fully understand how this enzyme works in a similar manner in all organisms. The K_M values for androstenedione are found to be in the nM range for all species where aromatase has been studied. This suggests that the enzyme is optimized for substrate binding. The ability of the enzyme to intrinsically stabilize different iron intermediates of the classical cytochromes P450 cycle acting in the three catalytic steps could be the reason why aromatase is well conserved among species where mainly one highly optimized isoform is present.

References.

[1] Thompson, E. A. Jr., Siiteri, P. K. (1974) The involvement of human placental microsomal cytochrome P-450 in aromatization. *J. Biol. Chem.* **249**, 5373-5378.

[2] Thompson, E. A. Jr., Siiteri, P. K. (1974) Utilization of oxygen and reduced nicotinamide adenine dinucleotide phosphate by human placental microsomes during aromatization of androstenedione. *J. Biol. Chem.* **249**, 5364-5372.

[3] Simpson, E., Mahendroo, M., Means, G., Kilgore, M., Hinshelwood, M., Graham-Lorence, S., Amarneh, B., Ito, Y., Fisher, C., Michael, M. (1994) Aromatase cytochrome P450, the enzyme responsible for estrogen biosynthesis. *Endocr. Rev.* **15**, 342-55.

[4] Baggett, B., Dorfman, R. I., Engel, L. L., Savard, K. (1956) The conversion of testosterone-3-C14 to C14-estradiol-17beta by human ovarian tissue. *J. Biol. Chem.* **221**, 931-941.

[5] Davis, J. W., Gut, M., Lemon, H. M., Wotiz, H. H. (1956) Studies in steroid metabolism. V. The conversion of testosterone-4-C14 to estrogens by human ovarian tissue. *J. Biol. Chem.* **222**, 487-495.

[6] Meyer, A. S. (1955) Conversion of 19-hydroxy-delta 4-androstene-3,17-dione to estrone by endocrine tissue. *Biochim. Biophys. Acta* **17**, 441-442.

[7] Ryan, K. J. (1959) Biological aromatization of steroids. *J. Biol. Chem.* **234**, 268-272.

[8] Harada, N. (1997) Aberrant expression of aromatase in breast cancer tissues. *J. Steroid. Biochem. Mol. Biol.* **61**, 175-184.

[9] Santen, R. J., Brodie, H., Simpson, E. R., Siiteri, P. K. Brodie, A. (2009) History of aromatase: saga of an important biological mediator and therapeutic target. *Endocr. Rev.* **30**, 343-375.

[10] Callard, G. V., Pudney, J. A., Kendall, S. L., Reinboth, R. (1984) In vitro conversion of androgen to estrogen in amphioxus gonadal tissues. *Gen. comp. endocrinol.* **56**, 53-58.

[11] Tchoudakova, A., Callard, G. V. (1998) Identification of multiple CYP19 genes encoding different cytochrome P450 aromatase isozymes in brain and ovary. *Endocrinology.* **139**, 2179-2189.

[12] Graddy, L. G., Kowalski, A. A., Simmen, F. A., Davis, S. L. F., Baumgartner, W. W., Simmen, R. C. M. (2000) Multiple isoforms of porcine aromatase are encoded by three distinct genes. *J. Steroid Biochem. Mol. Biol.* **73**, 49-57.

[13] Hong, Y., Li, H., Yuan, Y.C., Chen, S. (2009) Molecular characterization of aromatase. *Ann. N. Y. Acad. Sci.* **1155**, 112-120.

[14] Wilson, J. Y., McArthur, A. G., Stegeman, J. J. (2005) Characterization of a cetacean aromatase (CYP19) and the phylogeny and functional conservation of vertebrate aromatase. *Gen. Comp. Endocrinol.* **140**, 74-83.

[15] Hong, Y., Li, H., Yuan, Y.C., Chen, S. (2010) Sequence-function correlation of

aromatase and its interaction with reductase. *J. Steroid Biochem. Mol. Biol.* **118**, 203-206.

[16] McArthur, A. G., Hegelund, T., Cox, R. L., Stegeman, J. J., Liljenberg, M., Olsson, U., Sundberg, P., Celander, M. C. (2003) Phylogenetic analysis of the cytochrome P450 3 (CYP3) gene family. *J. Mol. Evol.* **57**, 200-211.

[17] Jenkins, V., Atkins, L., Fallowfield, L. (2007) Does endocrine therapy for the treatment and prevention of breast cancer affect memory and cognition? *Eur. J. Cancer.* **43**, 1342-1347.

[18] Conley, A., Hinshelwood, M. (2001) Mammalian aromatases. *Reproduction* **121**, 685-695.

[19] Simpson, E. R., Clyne, C., Rubin, G., Boon, W. C., Robertson, K., Britt, K., Speed, C. Jones, M. (2002) Aromatase - A brief overview. *Annu. Rev. Physiol.* **64**, 93-127.

[20] Chumsri, S., Howes, T., Bao, T., Sabnis, G., Brodie, A. (2011) Aromatase, aromatase inhibitors, and breast cancer. *J. Steroid Biochem. Mol. Biol.* **125**, 13-22.

[21] Naftolin, F., Ryan, K. J., Davies, I. J., Petro, Z., Kuhn, M. (1975) The formation and metabolism of estrogens in brain tissues. *Adv Biosci.* **15**, 105-121.

[22] Wagner, C., Morrell, J. (1997) Neuroanatomical distribution of aromatase mRNA in the rat brain: indications of regional regulation. *J. Steroid Biochem. Mol. Biol.* **61**, 307-314.

[23] MacLusky, N., Naftolin, F., Krey, L., Franks, S. (1981) The catechol estrogens. *J. Steroid Biochem.* **15**, 111-124.

[24] Roselli, C. F. (2007) Brain aromatase: roles in reproduction and neuroprotection. *J. Steroid Biochem. Mol. Biol.* **106**, 143-50.

[25] Lephart, E. D., Lund, T. D., Horvath, T. L. (2001) Brain androgen and progesterone metabolizing enzymes: biosynthesis, distribution and function. *Brain Res. Brain Res. Rev.* **37**, 25-37.

[26] McCullough, L. D., Blizzard, K., Simpson, E. R., Oz, O. K., Hurn, P. D. (2003) Aromatase cytochrome P450 and extragonadal estrogen play a role in ischemic neuroprotection. *J. Neurosci.* **23**, 8701-8705.

[27] Yue, X., Lu, M., Lancaster, T., Cao, P., Honda, S. I., Staufenbiel, M., Harada, N., Zhong, Z. Y., Shen, Y., Li, R. N. (2005) Brain estrogen deficiency accelerates A beta plaque formation in an Alzheimer's disease animal model, *Proc. Natl. Acad. Sci. USA* **102**, 19198-19203.

[28] Morale, M. C., L'Episcopo, F., Tirolo, C., Giaquinta, G., Caniglia, S., Testa, N., Aycieri, P., Serra, P. A., Lupo, G., Alberghina, M., Harada, N., Honda, S., Panzica, G. C., Marchetti, B. (2008) Loss of aromatase cytochrome P450 function as a risk factor for Parkinson's disease? *Brain Res. Rev.* **57**, 431-443.

[29] Combarros, O., Sanchez-Juan, P., Riancho, J. A., Mateo, I., Rodriguez-Rodriguez, E., Infante, J., Garcia-Gorostiaga, I., Vazquez-Higuera, J. L., Berciano, J. (2008) Aromatase and interleukin-10 genetic variants interactively modulate Alzheimer's disease risk. *J. Neural Transm.* **115**, 863-867.

[30] Cheng, Q., Sohl, C. D., Yoshimoto, F. K., Guengerich, F. P. (2012) Oxidation of dihydrotestosterone by human cytochromes P450 19A1 and 3A4. *J. Biol. Chem.* **287**, 29554-29567.

[31] Osawa, Y., Higashiyama, T., Shimizu, Y., Yarborough, C. (1993) Multiple functions of aromatase and the active site structure aromatase is the placental estrogen 2-hydroxylase. *J. Steroid Biochem. Mol. Biol.* **44**, 469-480.

[32] Brodie, H. J., Kripalani, K. J., Possanza, G. (1969) Studies on the mechanism of estrogen biosynthesis. VI. The stereochemistry of hydrogen elimination at C-2 during aromatization. *J. Am. Chem. Soc*. **91**, 1241-1242.

[33] Fishman, J., Guzik, H. (1969) Stereochemistry of estrogen biosynthesis. *J. Am. Chem. Soc*. **91**, 2805-2806.

[34] Fishman, J., Guzik, H., Dixon, D. (1969) Stereochemistry of estrogen biosynthesis. *Biochemistry* **8**, 4304-4309.

[35] Akhtar, M., Calder, M. R., Corina, D. L. & Wright, J. N. (1982) Mechanistic studies on C-19 demethylation in oestrogen biosynthesis. *Biochem. J.* **201**, 569-580.

[36] Hackett, J. C., Brueggemeier, R. W., Hadad, C. M. (2005) The final catalytic step of cytochrome P450 aromatase: A density functional theory study. *J. Am. Chem. Soc.***127**, 5224-5237.

[37] Ghosh, D., Griswold, J., Erman, M., Pangborn, W. (2009) Structural basis for androgen specificity and oestrogen synthesis in human aromatase. *Nature* **457**, 219-223.

[38] Sen, K., Hackett, J. C. (2012) Coupled electron transfer and proton hopping in the final step of CYP19-catalyzed androgen aromatization. *Biochemistry* **51**, 3039-3049.

[39] Sohl, C., Guengerich, F. (2010) Kinetic analysis of the three-step steroid aromatase reaction of human cytochrome P450 19A1. *J Biol. Chem*. **285**, 17734-43.

[40] Guengerich, F. P., Sohl, C. D., Chowdhury, G. (2011) Multi-step oxidations catalyzed by cytochrome P450 enzymes: processive vs. distributive kinetics and the issue of carbonyl oxidation in chemical mechanisms. *Arch. Biochem. Biophys.* **507**, 126-34.

[41] Zhou, D. J., Cam, L. L., Laughton, C. A., Korzekwa, K. R., Chen, S. (1994) Mutagenesis study at a postulated hydrophobic region near the active-site of aromatase cytochrome-P450. *J. Biol. Chem.* **269**, 19501- 19507.

[42] Kagawa, N., Cao, Q., Kusano, K. (2003) Expression of human aromatase (CYP19) in Escherichia coli by N-terminal replacement and induction of cold stress response. *Steroids.* **68**, 205-209.

[43] Fogli, M. V., Perozzo, R., Cavalli, A., Scapozza, L. (2003) Expression and purification of a new recombinant form of human aromatase in *Escherichia coli*. *Drug Metab. Rev.* **35**, 36.

[44] Kagawa, N., Hori, H., Waterman, M. R., Yoshioka, S. (2004) Characterization of stable human aromatase expressed in E. coli. *Steroids.* **69**, 235-243.

[45] Hong, Y., Yu, B., Sherman, M., Yuan, Y.C., Zhou, D., Chen, S. (2007) Molecular basis for the aromatization reaction and exemestane-mediated irreversible inhibition of human aromatase, *Mol. Endocrinol.* **21**, 401-414.

[46] Kagawa, N. (2011) Efficient expression of human aromatase (CYP19) in E. coli. *Methods Mol. Biol.* **705**, 109-122.

[47] Sigle, R. O., Titus, M. A., Harada, N. & Nelson, S. D. (1994) Baculovirus-mediated high-level expression of human placental aromatase (CYP19A1). *Biochem. Biophys. Res. Commun.* **201**, 694-700.

[48] Amarneh, B., Simpson, E. R. (1995) Expression of a recombinant derivative of human aromatase P450 in insect cells utilizing the baculovirus vector system. *Mol. Cell. Endocrinol.* **109**, 1-5.

[49] Zhang, F., Zhou, D., Kao, Y., Ye, J., Chen, S. (2002) Expression and purification of a recombinant form of human aromatase from Escherichia coli. *Biochem. Pharmacol.* **64**, 1317-24.

[50] Tosha, T., Kagawa, N., Ohta, T., Yoshioka, S., Waterman, M. R., Kitagawa, T. (2006) Raman evidence for specific substrate-induced structural changes in the heme pocket of human cytochrome P450 aromatase during the three consecutive oxygen activation steps. *Biochemistry* **45**, 5631-5640.

[51] Grinkova, Y. V., Denisov, I. G., Waterman, M. R., Arase, M., Kagawa, N., Sligar,

S. G. (2008) The ferrous-oxy complex of human aromatase. *Biochem. Biophys. Res. Comm.* **372**, 379-382.

[52] Maurelli, S., Chiesa, M., Giamello, E., Di Nardo, G., Ferrero, V. E. V., Gilardi, G., Van Doorslaer, S. (2011) Direct spectroscopic evidence for binding of anastrozole to the iron heme of human aromatase. Peering into the mechanism of aromatase inhibition. *Chem. Comm.* **47**, 10737- 10739.

[53] Denisov, I. G., Grinkova, Y. V., McLean, M. A., Sligar, S. G. (2007) The one-electron autoxidation of human cytochrome P450 3A4. *J. Biol. Chem.* **282**, 26865-26873.

[54] Gantt, S. L., Denisov, I. G., Grinkova, Y. V., Sligar, S. G. (2009) The critical iron-oxygen intermediate in human aromatase. *Biochem. Biophys. Res. Comm.* **387**, 169-173.

[55] Denisov, I. G., Makris, T. M., Sligar, S. G., Schlichting, I. (2005) Structure and chemistry of cytochrome P450. *Chem. Rev.* **105**, 2253- 2277.

[56] Sligar, S. G., Lipscomb, J. D., Debrunner, P. G., Gunsalus, I. C. (1974) Superoxide anion production by the autoxidation of cytochrome P450cam. *Biochem. Biophys. Res. Comm.* **61**, 290-296.

[57] Luthra, A., Denisov, I. G., Sligar, S. G. (2011) Temperature derivative spectroscopy to monitor the autoxidation decay of cytochromes P450. *Anal. Chem.* **83**, 5394-5399.

[58] Davydov, R., Makris, T. M., Kofman, V., Werst, D. E., Sligar, S. G., Hoffman, B. M. (2001) Hydroxylation of camphor by-reduced oxy-cytochrome P450cam: Mechanistic implications of EPR and ENDOR studies of catalytic intermediates in native and mutant enzymes. *J. Am. Chem. Soc.* **123**, 1403-1415.

[59] Davydov, R., Razeghifard, R., Im, S.C., Waskell, L., Hoffrnan, B. M. (2008) Characterization of the microsomal cytochrome P4502B4O(2) activation intermediates by cryoreduction and electron paramagnetic resonance. *Biochemistry* **47**, 9661-9666.

[60] Ghosh, D., Lo, J., Morton, D., Valette, D., Xi, J., Griswold, J., Hubbell, S., Egbuta, C., Jiang, W., An, J., Davies, H. M. L. (2012) Novel aromatase inhibitors by structure-guided design. *J. Med. Chem.* **55**, 8464-8476.

[61] Kao, Y. C., Cam, L. L., Laughton, C. A., Zhou, D. J., Chen, S. A. (1996) Binding characteristics of seven inhibitors of human aromatase: A site-directed mutagenesis study. *Cancer Res.* **56**, 3451- 3460.

[62] Kao, Y. C., Korzekwa, K. R., Laughton, C. A., Chen, S. (2001) Evaluation of the mechanism of aromatase cytochrome P450 - A site-directed mutagenesis study. *Eur. J. Biochem.* **268**, 243-251.

[63] Auvray, P., Nativelle, C., Bureau, R., Dallemagne, P., Seralini, G. E., Sourdaine, P. (2002) Study of substrate specificity of human aromatase by site directed mutagenesis, *Eur. J. Biochem.* **269**, 1393-13405.

[64] Kadohama, N., Yarborough, C., Zhou, D., Chen, S., Osawa, Y. (1992) Kinetic properties of aromatase mutants Pro308Phe, Asp309Asn, and Asp309Ala and their interactions with aromatase inhibitors. *J. Steroid Biochem. Mol. Biol.* **43**, 693-701.

[65] Hong, Y., Cho, M., Yuan, Y.C. Chen, S. (2008) Molecular basis for the interaction of four different classes of substrates and inhibitors with human aromatase. *Biochem. Pharmacol.* **75**, 1161- 1169.

[66] Bernhardt, R., Pommerening, K., Ruckpaul, K. (1987) Modification of carboxyl groups on nadph-cytochrome-p-450 reductase involved in binding of cytochromes-c and P-450 LM2. *Biochem. Int.* **14**, 823-832.

[67] Bernhardt, R., Kraft, R., Otto, A., Ruckpaul, K. (1988) Electrostatic interactions between cytochrome-P-450 LM2 and NADPH-cytochrome-P-450 reductase. *Biomed. Biochim. Acta.* **47**, 581-592.

[68] Nadler, S. G., Strobel, H. W. (1988) Role of electrostatic interactions in the reaction of NADPH-cytochrome P-450 reductase with cytochromes P-450. *Arch. Biochem. Biophys.* **261**, 418-429.

[69] Hong, Y., Rashid, R., Chen, S. (2011) Binding features of steroidal and nonsteroidal inhibitors. *Steroids.* **76**, 802-806.

[70] Sevrioukova, I. F., Li, H. Y., Zhang, H., Peterson, J. A., Poulos, T. L. (1999) Structure of a cytochrome P450-redox partner electron-transfer complex. *Proc. Natl. Acad. Sci. USA* **96**, 1863-1868.

[71] Shimizu, T., Tateishi, T., Hatano, M., Fujiikuriyama, Y. (1991) Probing the role of lysines and arginines in the catalytic function of cytochrome-P450d by site-directed mutagenesis - interaction with NADPH-cytochrome-p450 reductase. *J. Biol. Chem.* **266**, 3372- 3375.

[72] Stayton, P. S., Sligar, S. G. (1990) The cytochrome-P-450cam binding surface as defined by site-directed mutagenesis and electrostatic modeling. *Biochemistry* **29**, 7381-7386.

[73] Hong, Y., Li, H., Ye, J., Miki, Y., Yuan, Y.C., Sasano H., Evans, D.B., Chen, S.

(2009) Epitope characterization of an aromatase monoclonal antibody suitable for the assessment of intratumoral aromatase activity. *PLoS One* **4**, e8050.
[74] Catalano, S., Barone, I., Giordano, C., Rizza, P., Qi, H., Gu, G., Malivindi, R., Bonofiglio, D., Andò, S. (2009) Rapid estradiol/ER alpha signaling enhances aromatase enzymatic activity in breast cancer cells. *Mol. Endocrinol.* **23**, 1634-1645.
[75] Ghosh, D., Jiang, W., Lo, J., Egbuta, C. (2011) Higher order organization of human placental aromatase. *Steroids* **76**, 753-758.
[76] Shimozawa, O., Sakaguchi, M., Ogawa, H., Harada, N., Mihara, K., Omura, T. (1993) Core glycosylation of cytochrome-P-450 (arom) - evidence for localization of N-terminus of microsomal cytochrome-P-450 in the lumen. *J. Biol. Chem.* **268**, 21399-21402.
[77] Jiang, W., Ghosh, D. (2012) Motion and flexibility in human cytochrome P450 aromatase. *Plos One* **7**, e32565.
[78] Sgrignani, J., Magistrato, A. (2012) Influence of the membrane lipophilic environment on the structure and on the substrate access/egress routes of the human aromatase enzyme. A computational study. *J. Chem. Inf. Model.* **52**, 1595-1606.
[79] Cojocaru, V., Winn, P. J., Wade, R. C. (2007) The ins and outs of cytochrome P450s. *Biochim. Biophys. Acta* **1770**, 390-401.

Tables.

Table 1. Summary of the changes (%) in the catalytic parameters toward the substrate androstenedione for selected site directed mutants of aromatase respect to the WT enzyme.

Residue	Location/role	Mutant	K_M (%)	V_{MAX} (%)	Ref.
		WT	100	100	
K119	Helix B	K119T	<1	<1	[63]
		K119Y	287	106	[63]
		K119V	109	159	[63]
		K119E	34	133	[63]
G121	Helix B	G121A	33.7[a] 38.9[b]	28.8[a] 125[b]	[41]
C124	Helix B	C124Y	91	49	[63]
I125	Helix B	I125N	84.9[a]	10.5[a]	[41]
K130	B-C loop	K130N	89	81	[63]
I133	B-C loop / van der Waals contact with substrate	I133Y	29[a] 2250[b]	2.2[a] 3.7[b]	[61]
		I133W	136[a] 1937.5[b]	<1[a] <1[b]	[61]
F221	Helix F / van der Waals contact with substrate	F221Y	10.6	22.9	[69]
W224	Helix F / van der Waals contact with substrate	W224F	245.4	22.3	[69]
F235	Helix G'	F235L	96.7[a] 181.25[b]	26.3[a] 11.1[b]	[61]
I395	β-sheet 1, strand 6	I395F	16.1[a] 3312.5[b]	9.5[a] 25.9[b]	[61]
E302	Helix I	E302D	110.3[a]	15.2[a]	[62]

			203.3[b]	7.9[b]	
		E302A	<1	<1	[63]
P308	Helix I / Distorsion in helix to allow substrate accomodation	P308F	51.6[a] 293.8[b] 25.9	9.5[a] 51.9[b] 9.1	[41,61,64]
D309	Helix I / Hydrogen bond with the substrate	D309A	<1	<1	[41,61,64]
		D309A	74[a] 2156[b]	1.5[a] 14.8[b]	[63]
T310	Helix I / Part of the catalytic cleft	T310S	103[a] 93.8[a]	17.5[a] 14.8[b]	[61]
F320	Helix I	F320C	67	69	[63]
I361	Helix K	Y361F	87.6	76.0	[41]
		Y361L	79.7	67.6	[41]
M374	β-sheet 1, strand 3 / van der Waals contact with substrate	M374T	65.2	8.5	[69]
I395	β-sheet 1, strand 6	I395F	16.1[a] 33125[b]	9.4[a] 25.9[b]	[61]
S470	β7- β10 loop	S470N	176	80	[63]
I471	β7- β10 loop	I471M			[63]
I474	β-sheet 3, strand 8	I474Y	38.7[a] 87.5[b]	17.5[a] 11.1[b]	[61]
		I474W	80.6[a] 87.5[a]	6.6[a] 11.1[b]	[61]
		I474M	<15	<15	[61]
		I474N	22.5[a] 1168.8[b]	25.5[a] 22.2[b]	[61]

		I474T	386	135	[63]
		I474F	60.5[a] 34.7[b]	81.4[a] 106.3[b]	[41]
H475	β-sheet 3, strand 8	H475N	<5	<5	[63]
		H475R	<5	<5	[63]
		H475A	41	78	[63]
		H475E	<5	<5	[63]
D476	β8- β9 loop	D476A	<1	<1	[63]
		D476K	<1	<1	[63]
		D476L	<5	<5	[63]
		D476N	113	56	[63]
		D476E	76	87	[63]
S478	β8- β9 loop	S478A	84.7[a] 116.6[b]	69.6[a] 24.7[b]	[62]
		S478T	18[a] 56.7[b]	16.4[a] 18.8[b]	[62]
H480	β-sheet 3, strand 9	H480K	51.7[a] 128.8[b]	30.6[a] 90[b]	[62]
		H480Q	9.9[a] 43.6[b]	9.7[a] 12[b]	[62]

[a] data from “in-cell” assay

[b] data from microsomal assay

Figure legends.

Figure 1. Molecular structure of the androgen substrates of aromatase and the corresponding estrogen products.

Figure 2. Mechanisms proposed for the third step of the reaction catalysed by aromatase. A) The ferric peroxide species of the P450 ($FeOO^-$) gives a nucleophilic attack to the carbonyl group of the aldehyde with a consequent peroxide fragmentation and abstraction of the 1*β* proton (adapted from [35]). B) The "Compound I" is responsible for 1*β*-hydrogen subtraction from a *gem*-diol intermediate, followed by an electron transfer from the A-ring to the iron ($Fe^{3+}OH$) and the subtraction of a second hydrogen from the steroid molecule (adapted from [36]). C) The ferric peroxide species of the P450 ($FeOO^-$) attacks the aldehyde causing the cleavage of the C10-C19 bond through the formation of a peroxohemiacetal and peroxoformate intermediates. The cleavage of the O-O bond causes formate extrusion with a concomitant formation of Compound II ($Fe^{3+}OH$) by 1*β*-hydrogen abstraction, which removes the 2*β*-hydrogen (adapted from [38]).

Figure 3. Active site of human aromatase (PDB ID: 3EQM) with heme shown in red and the substrate androstenedione in cyan. The residues targeted for mutagenesis studies are shown in stick representation. Mutations of Phe221, Trp224, Pro308, Asp309, Thr310 and Met374 resulted in a decrease of k_{cat} values for androstenedione turnover. Mutation of Trp224 and Asp309 also were shown to increase K_M values for androstenedione.

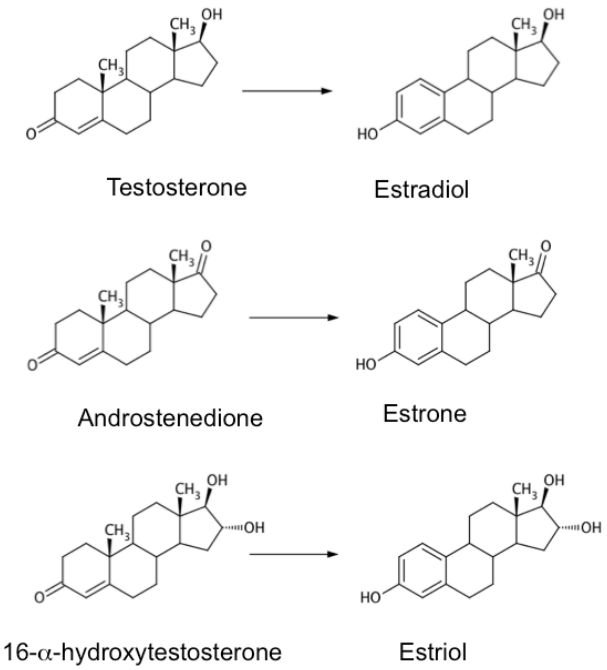
Testosterone
Estradiol
Androstenedione
Estrone
16-α-hydroxytestosterone
Estriol

FIGURE 1

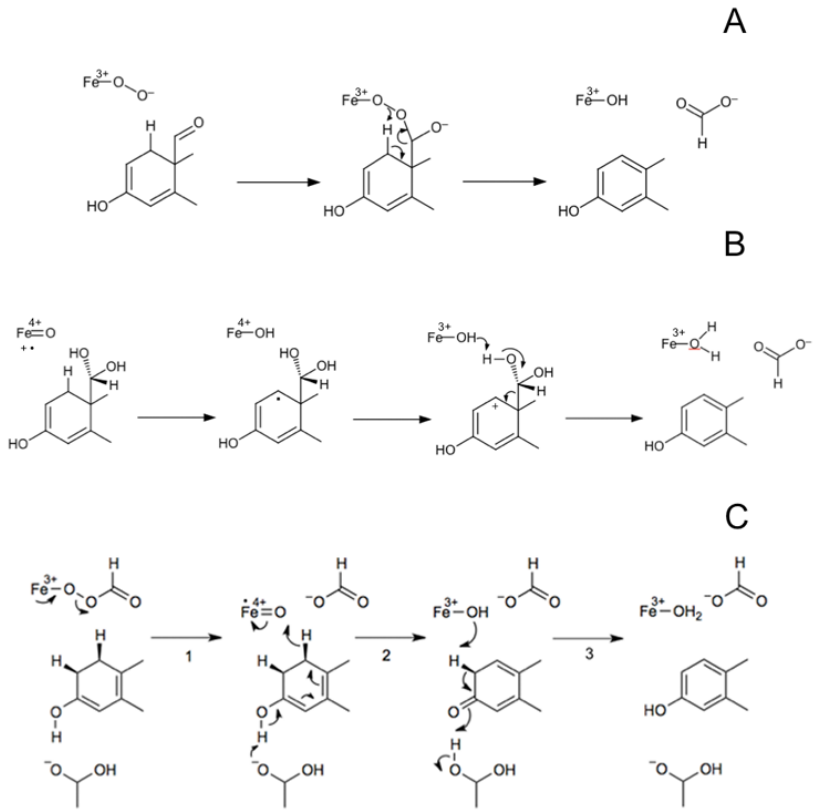
A
B
C
1
2
3

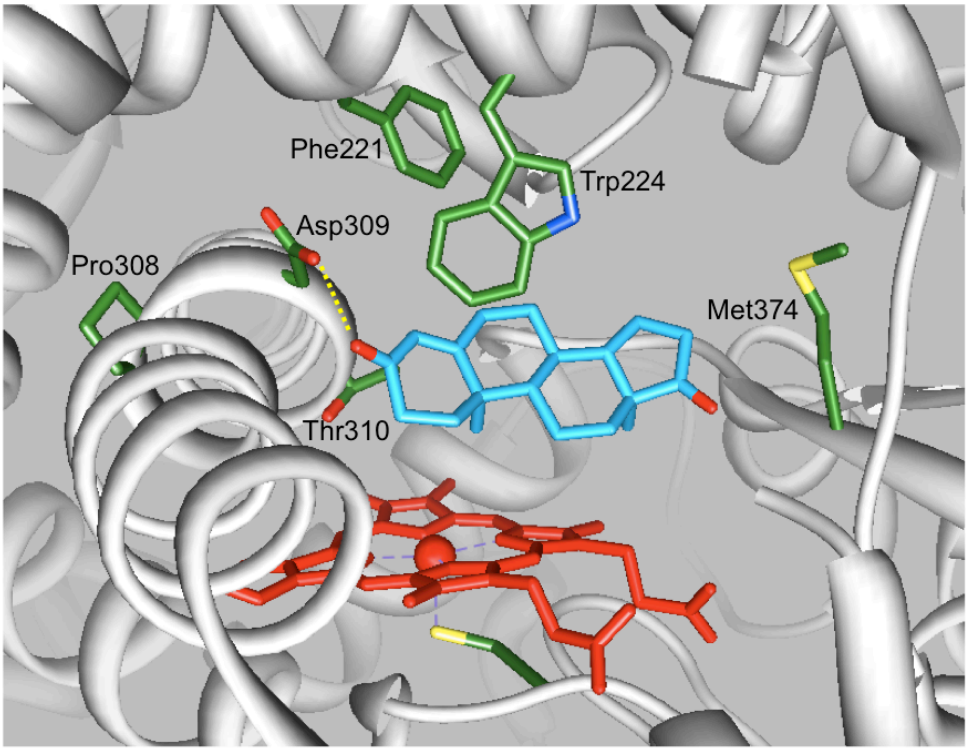

FIGURE 3